



# Full-circle range and microradian resolution angle measurement using the orthogonal mirror self-mixing interferometry

CHENCHEN WANG,<sup>1</sup> XUEWEI FAN,<sup>1</sup> YOU GUO,<sup>1</sup> HUAQIAO GUI,<sup>2</sup> HUANQING WANG,<sup>3</sup> JIANGUO LIU,<sup>2</sup> BENLI YU,<sup>1</sup> AND LIANG LU<sup>1,\*</sup>

<sup>1</sup> Key Laboratory of Opto-Electronic Information Acquisition and Manipulation of Ministry of Education, Anhui University, Jiulong Road 111#, Hefei, 230601, China

<sup>2</sup> Key Laboratory of Environmental Optics and Technology, Anhui Institute of Optics and Fine Mechanics, Chinese Academy of Sciences, Hefei 230031, China

<sup>3</sup> State Key Laboratory of Transducer Technology, Institute of Intelligent Machines, Chinese Academy of Sciences, 350 Shu Shang Hu Road, Hefei, 230031, China

\*lianglu@ahu.edu.cn

**Abstract:** The self-mixing technique based on the traditional reflecting mirror has been demonstrated with great merit for angle sensing applications. In order to solve the problems of the narrow measurement angle range and low resolution in traditional angle measurement method, we proposed an angle measurement system using orthogonal mirror self-mixing interferometry combine an orthogonal mirror with designed mechanical linkage. It overcomes the shortcomings of traditional angle measurement methods and realized the angle measurement with microradian resolution in a full-circle range of 0 rad to  $2\pi$  rad. In the experiment, the measurement resolution can reach to 5.27  $\mu$ rad and the absolute error can lower to  $\pm 0.011\mu$ rad, which satisfies the requirements of most high accuracy angle measurement.

© 2018 Optical Society of America under the terms of the [OSA Open Access Publishing Agreement](#)

**OCIS codes:** (280.3420) Laser sensors; (350.4600) Optical engineering.

## References and links

1. N. A. Emadi, L. B. Brahim, and M. Benammar, "A new tracking technique for mechanical angle measurement," *Measurement* **54**(8), 58–64 (2014).
2. B. Yang, D. Wang, L. Zhou, S. Wu, R. Xiang, W. Zhang, H. Gui, J. Liu, H. Wang, L. Lu, and B. Yu, "A ultra-small-angle self-mixing sensor system with high detection resolution and wide measurement range," *Opt. Laser Technol.* **91**, 92–97 (2017).
3. P. R. Yoder, Jr., E. R. Schlesinger, and J. L. Chickvary, "Active annular-beam laser autocollimator system," *Appl. Opt.* **14**(8), 1890–1895 (1975).
4. P. S. Huang, S. Kiyono, and O. Kamada, "Angle measurement based on the internal-reflection effect: a new method," *Appl. Opt.* **31**(28), 6047–6055 (1992).
5. M. Dobosz and O. Iwasinska-Kowalska, "Interference method for ultra-precision measurement and compensation of laser beam angular deflection," *Appl. Opt.* **53**(1), 111–122 (2014).
6. A. Zhang and P. S. Huang, "Total internal reflection for precision small-angle measurement," *Appl. Opt.* **40**(10), 1617–1622 (2001).
7. J. Y. Lin and Y. C. Liao, "Small-angle measurement with highly sensitive total-internal-reflection heterodyne interferometer," *Appl. Opt.* **53**(9), 1903–1908 (2014).
8. Y. Pavan Kumar, S. Chatterjee, and S. S. Negi, "Small roll angle measurement using lateral shearing cyclic path polarization interferometry," *Appl. Opt.* **55**(5), 979–983 (2016).
9. F. Cheng and K. C. Fan, "High-resolution angle measurement based on michelson interferometry," *Phys. Procedia* **19**(19), 3–8 (2011).
10. J. Zhong, X. Zhang, and Z. Ju, "Absolute small-angle measurement based on optical feedback interferometry," *Chin. Opt. Lett.* **6**(11), 830–832 (2008).
11. S. Zhang, Y. Tan, and S. Zhang, "Non-contact angle measurement based on parallel multiplex laser feedback interferometry," *Chin. Phys. B* **23**(11), 114202 (2014).
12. J. Yuan and X. Long, "CCD-area-based autocollimator for precision small-angle measurement," *Rev. Sci. Instrum.* **74**(3), 1362–1365 (2003).
13. A. E. Ennos and M. S. Virdee, "High accuracy profile measurement of quasi-conical mirror surface by laser autocollimation," *Precis. Eng.* **4**(1), 5–8 (1982).

14. K. Zhu, B. Guo, S. Zhang, Y. Tan, and Y. Tan, "Single-spot two-dimensional displacement measurement based on self-mixing interferometry," *Optica* **4**(7), 729–735 (2017).
15. S. Donati, D. Rossi, and M. Norgia, "Single channel self-mixing interferometer measures simultaneously displacement and tilt and yaw angles of a reflective target," *IEEE J. Quantum Electron.* **51**(12), 1400108 (2015).
16. D. Guo and M. Wang, "Self-mixing interferometry based on a double-modulation technique for absolute distance measurement," *Appl. Opt.* **46**(9), 1486–1491 (2007).
17. S. Zhang, L. Yan, B. Chen, Z. Xu, and J. Xie, "Real-time phase delay compensation of PGC demodulation in sinusoidal phase-modulation interferometer for nanometer displacement measurement," *Opt. Express* **25**(1), 472–485 (2017).
18. Y. Wei, W. Huang, Z. Wei, J. Zhang, T. An, X. Wang, and H. Xu, "Double-path acquisition of pulse wave transit time and heartbeat using self-mixing interferometry," *Opt. Commun.* **393**, 178–184 (2017).
19. J. Chen, H. Zhu, W. Xia, D. Guo, H. Hao, and M. Wang, "Self-mixing birefringent dual-frequency laser Doppler velocimeter," *Opt. Express* **25**(2), 560–572 (2017).
20. S. Wu, D. Wang, R. Xiang, J. Zhou, Y. Ma, H. Gui, J. Liu, H. Wang, L. Lu, and B. Yu, "All-fiber configuration laser self-mixing doppler velocimeter based on distributed feedback fiber laser," *Sensors (Basel)* **16**(8), 1179 (2016).
21. Y. L. Lim, R. Kliese, K. Bertling, K. Tanimizu, P. A. Jacobs, and A. D. Rakić, "Self-mixing flow sensor using a monolithic VCSEL array with parallel readout," *Opt. Express* **18**(11), 11720–11727 (2010).
22. S. Sudo, T. Ohtomo, Y. Takahashi, T. Oishi, and K. Otsuka, "Determination of velocity of self-mobile phytoplankton using a self-mixing thin-slice solid-state laser," *Appl. Opt.* **48**(20), 4049–4055 (2009).
23. X. Dai, M. Wang, Y. Zhao, and J. Zhou, "Self-mixing interference in fiber ring laser and its application for vibration measurement," *Opt. Express* **17**(19), 16543–16548 (2009).
24. U. Zabit, F. Bony, T. Bosch, and A. D. Rakić, "A self-mixing displacement sensor with fringe-loss compensation for harmonic vibrations," *IEEE Photonic. Tech. Lett.* **22**(6), 410–412 (2010).
25. W. M. Wang, K. T. V. Grattan, A. W. Palmer, and W. J. O. Boyle, "Self-mixing interference inside a single-mode diode laser for optical sensing applications," *J. Lightwave Technol.* **12**(9), 1577–1587 (1994).
26. W. M. Wang, W. J. Boyle, K. T. Grattan, and A. W. Palmer, "Self-mixing interference in a diode laser: experimental observations and theoretical analysis," *Appl. Opt.* **32**(9), 1551–1558 (1993).
27. P. J. de Groot, G. M. Gallatin, and S. H. Macomber, "Ranging and velocimetry signal generation in a backscatter-modulated laser diode," *Appl. Opt.* **27**(21), 4475–4480 (1988).

## 1. Introduction

Angle measurement technology including mechanical angle measuring technology [1], electromagnetic angle measuring technology and optical angle measuring technology [2–11] is needed for many industrial applications, such as optical collimation, precision machining [2,3,12]. Compared with the shortcoming of mechanical and electromagnetic angle measuring technology that need manual operation and contact measurement, the optical angle measuring technology like auto-collimatic method [3, 13], total internal reflection method [4–7], and laser interferometry method [7–11] is most extensive used due to its advantages of non-contact measurement, strong electromagnetic immunity ability, high measurement accuracy and resolution.

For the requirements of compact structure, there are many angle measurement method based on self-mixing effect that is broadly used in measurement of displacements [14, 15–18], velocities [19–22] and vibration [23,24]. Laser self-mixing interferometry (SMI) angle measurement [2, 10,11] is optimal in numerous optical angles measuring techniques on account of its characteristic of single optical path, less optical components and self-aligned. However, traditional SMI method of angle measurement no matter with a rectangular prism [2] or with a reflecting mirror [10] both has a very strict limitation on the location of the incidence point due to the back-reflected light re-enter the laser cavity will be reduced or even disappear in case of the angle measured is slightly larger with the angle measurement resolution and range of angle measurement gradually reduced.

All the weakness of traditional SMI method above has inspired many researchers, including us, to attempt to create an improved angle measurement system aim to solve the problems that traditional SMI method encountered. In this paper, an effective method is proposed for full-circle range in order to overcome those issues that the traditional SMI method met. In our experiment, we build the angle measurement using orthogonal mirror self-mixing interferometry (AM-OM-SMI) system. Unlike the narrow measurement angle range in traditional SMI [2, 10-11], we realized angle measurement at full-circle range by using

designed mechanical linkages. In section 2, the theoretical analysis and numerical simulations of AM-OM-SMI system are demonstrated, the related experimental setup and result are given in Section 3 and 4, which are in good agreement with the theoretical analysis in Section 2. Finally, conclusions are drawn in Section 5.

## 2. System design and working principle of AM-OM-SMI

In this section, we proposed a basic theoretical model and theoretical simulation of AM-OM-SMI system. During the process of operating the AM-OM-SMI system, we use an orthogonal mirror as a key component of the experimental setup. An orthogonal mirror is placed in rotary disk to adjust experimental setup flexible. It can generate SMI signal with arbitrary location of incidence point by reflection property of orthogonal mirror, which avoid limitation on the location of the incidence point in traditional SMI method. The designed mechanical linkage that we used in experiment ensures light can re-enter the laser cavity along the original path at any measuring angle. In order to get the measurement resolution and range in our system, we attempt to study the Optical Path Difference (OPD) in AM-OM-SMI system caused by angle changed firstly. Figure 1 shows the principle schematic of the optical path of external cavity length in AM-OM-SMI system.

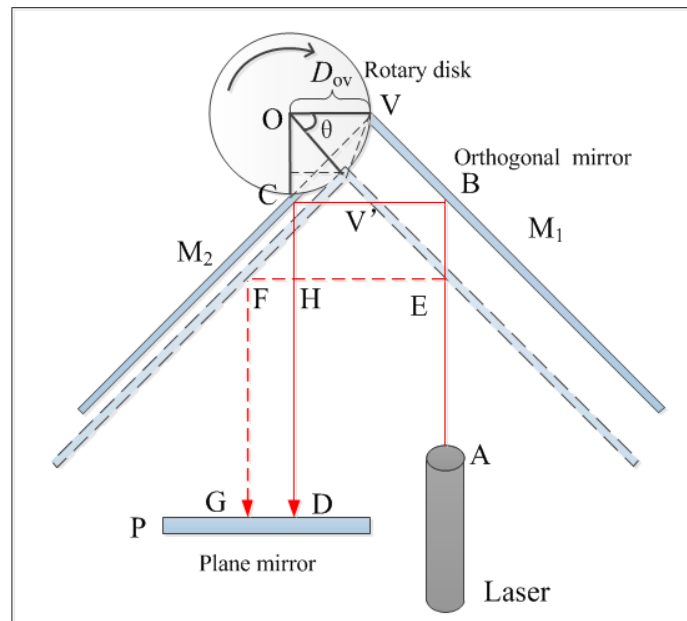


Fig. 1. The principle schematic of the optical path of external cavity length in AM-OM-SMI system.

As shown in Fig. 1, in initial position, an orthogonal mirror is placed in the rotary disk and  $OV$  (the line connecting the center point  $O$  of the rotary disk and the vertex point  $V$  of orthogonal mirror defined with the length of  $D_{ov}$ ) is parallel to the horizontal line. The light emitted from the laser incident on the orthogonal mirror at point  $B$  and reflected by the orthogonal mirror and plane mirror  $P$  then re-enter to the laser along the original optical path. Thus, the whole optical path of external cavity length in AM-OM-SMI system can be record as ABCDCBA. With the change of measuring angle, the vertex point of orthogonal mirror changes in corresponding. As the angle value is  $\theta$ , the vertex point of orthogonal mirror changes from point  $V$  to point  $V'$  and the initial optical path ABCDCBA has change into AEFGFEA. Combining the change of optical path discussed above with the schematic of the optical path in Fig. 1, the OPD can be deduced as follows:

$$\begin{aligned}
 OPD &= |n\Delta L| = |n(L_{AEFGFEA} - L_{ABCDCEA})| = |2n(FH - 2BE)| \\
 &= |-4nD_{ov} \sin \theta| = |2n(L_{ext} - L_0)|
 \end{aligned} \tag{1}$$

where  $n$  is air refractive index ( $n = 1$ );  $L_{ext}$  is the external cavity length;  $L_0$  is initial external cavity length. Owing to the length of external cavity length that introduced by the measurement angle is changed, the self-mixing effect could occurs when the the feedback light injected laser cavity and mixing with the light inside the cavity, causing the modulation of lasing frequency and output. Thus, the intensity of self-mixing angle signal can be described as follows based on the self-mixing interference theory of three-mirror Fabry-Perot cavity [25–27].

$$I = I_0[1 + m \cdot \cos(\varphi_L)] \tag{2}$$

where,  $I$ ,  $I_0$  is output intensity of laser with feedback light and without feedback light respectively;  $m$  is modulation coefficient of the interference ;  $\varphi_L$  is the phase of output laser with feedback light, it can be expressed as:

$$\varphi_L = \varphi_0 - C \sin(\varphi_0 + \arctan \alpha) \tag{3}$$

$$\varphi_0 = \frac{4\pi n L_{ext}}{\lambda} \tag{4}$$

here,  $\varphi_0$  is the phase of output laser without feedback light respectively;  $C$  is optical feedback coefficient;  $\alpha$  is linewidth enhancement factor;  $\lambda$  is laser output wavelength.

According to the self-mixing interference theory of three-mirror Fabry-Perot cavity proposed above [25–27], the self-mixing signal can generate a fringe when the optical path changes a wavelength of laser source. Thus, the relationship between fringe number and OPD can deduced further as follow:

$$OPD = |-4nD_{ov} \sin(\theta + \theta_0)| = N\lambda \tag{5}$$

where  $N$  is the fringe numbers;  $\theta_0$  is the initial angle of the orthogonal mirror. From Eq. (5), it shows that the measurable angle between the adjacent fringes is determined by the vertex distance  $D_{ov}$  and the sine value of the measured angle. Moreover, the angle between the adjacent fringes is the measurement resolution exactly in AM-OM-SMI system. Consequently, the measurement resolution can expressed as follow:

$$\theta_r = \arcsin\left(\left|-\frac{N\lambda}{4nD_{ov}}\right|\right) - \arcsin\left(\left|-\frac{(N-1)\lambda}{4nD_{ov}}\right|\right) \tag{6}$$

here,  $\theta_r$  is resolution of the angle measurement. On the basis of the above equations, a simulation of laser output power fluctuation caused by the angle changed was carried out. The simulated self-mixing signals with different vertex distance  $D_{ov}$  are shown in Fig. 2.

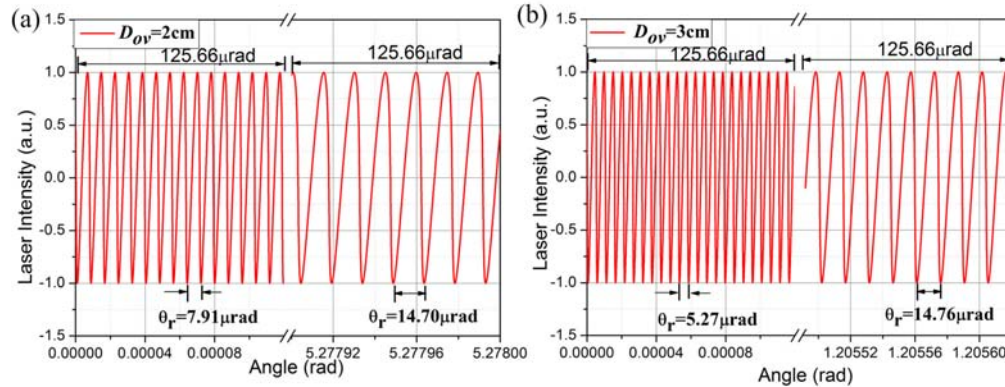


Fig. 2. Simulated self-mixing angle measurement signal with different vertex distance  $D_{ov}$ ,  $C$  is 0.8;  $\alpha$  is 3,  $\lambda$  is 632.8nm; (a) the vertex distance  $D_{ov} = 2$ cm; (b) the vertex distance  $D_{ov} = 3$ cm.

In order to make the reader get more information of the self-mixing angle signal in simulation, the Fig. 2 not only shows the simulated self-mixing signal with different vertex distance, but also provides the self-mixing signal in small starting angle and big starting angle under the same angle change range of  $125.66 \mu\text{rad}$ . The Fig. 2(a) is simulated self-mixing signals in starting angle of 0 rad and  $5.27787$  rad under the same angle change range with the vertex distance is 2 cm. Figure 2(b) is simulate self-mixing signals starting angle of 0 rad and  $1.20549$  rad under the same angle change range with vertex distance is 3cm. From Fig. 2(a) and Fig. 2(b), it shows that the fringe numbers is changed in different measured angle even under same angle change range, which affected the signal frequency and the angle measurement resolution corresponding. As two angle measurement resolutions in different measurement angle we marked in Fig. 2(a) and Fig. 2(b), the angle measurement resolution is  $7.91 \mu\text{rad}$  and  $5.27 \mu\text{rad}$  in small starting angle with the vertex distance is 2 cm and 3 cm respectively. The measurement resolution is  $14.70 \mu\text{rad}$  and  $14.76 \mu\text{rad}$  in big starting angle with the vertex distance is 2 cm and 3 cm respectively. Additionally, the fringe number in Fig. 2(b) is more than it in Fig. 2(a), which shows that the larger vertex distance, the higher resolution of the angle measurement system.

To further analyze the resolution more specifically, we simulate the angle measurement resolution at different measured angle of AM-OM-SMI system based on Eq. (6) in Fig. 3.

Figure 3 is the theoretical angle measurement resolution in the full-circle angle range ( $0-2\pi$ ) with different vertex distance. It could divide into four regions corresponding to four quadrant interval of a sinusoidal function with color of different gray level. Inset on the middle is enlarged Fig. of the black circle in the lower left corner of Fig. 3. Seen from the Fig. 3, the resolution in Region I and Region III is gradually increased, which is opposite of Region II and Region IV that decreased gradually. To analysis the angle measurement resolution precisely, we enlarge the black circle in the lower left corner of Region I in inset. It shows the best angle measurement resolution is  $7.91 \mu\text{rad}$  and  $5.27 \mu\text{rad}$  with different vertex distance. In addition, we also marked the worst angle measurement resolution in Fig. 3, it shows that the worst angle measurement resolution is  $416.99 \mu\text{rad}$  and  $279.01 \mu\text{rad}$  when the angle near  $\pi/2$  and  $3\pi/2$ , which is still better than the measurement resolution that traditional method has. In consequence, we made a Table 1 to clearly compare measurement range and best resolution to other angle measurement system, which shows the better performance than other measurement method.

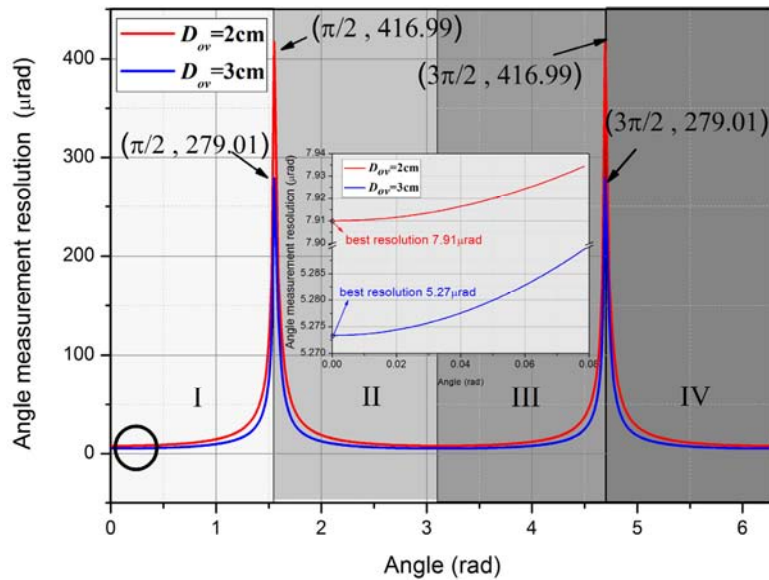


Fig. 3. Theoretical angle measurement resolution at different measuring angle.

Table 1. The comparison of measurement range and best resolution with other systems.

	Ref [2].	Ref [10].	Ref [11].	Our method
Measurement range / (rad)	$\pi/2$	0.0014	0.00678	$2\pi$
Best resolution / (rad)	$4.9 \times 10^{-4}$	$10^{-6}$	$2.42 \times 10^{-7}$	$5.27 \times 10^{-6}$

As shown in Table 1, the angle measurement range in this paper is the largest, which even can realize the angle measurement in full-circle range. As for the best resolution, it can lower to  $5.27 \mu\text{rad}$  that satisfied the requirements of most angle measurement.

### 3. Schematic of the experimental setup

For the sake of verifying the feasibility of utilizing the laser self-mixing principle to measure angle, experiments based on AM-OM-SMI have been made. The experimental setup based on orthogonal mirror and designed rotary mechanical linkage is shown in Fig. 4. In our experiment, AM-OM-SMI system composed of a He-Ne laser (CVI Melles Griot: 25-STP-912-230) with wavelength of 632.8nm, optical path adjustable part, signal collection part and target. Where, optical path regulating part is made up of variable optical attenuator, beam splitter and a reflector that marked plane mirror P in Fig. 1. Photoelectric detector (Thorlabs: PDA36A-EC), data acquisition card (National Instrument: PXI-1082) and computer constitutes whole signal collection part. The target is consisting of orthogonal mirror and designed mechanical linkage, which mainly used to change the measurement angle. As shown in Fig. 4, the variable optical attenuator was inserted into the external cavity to modify the feedback level for obtaining the optimal self-mixing signal. The beam splitter split the light emitted from the He-Ne laser into two beams, one of which is incident on the target and the other is received by the photoelectric detector. The beam incident on the target was reflected by orthogonal mirror that fixed on the orthogonal holder then incident on the reflector. Finally, the beam was reflected by the reflector and re-enter to the laser cavity to generate the self-mixing signal. In whole experiment, the data acquisition card is used to acquire the self-mixing signal then input the data into the computer to perform subsequent data processing.

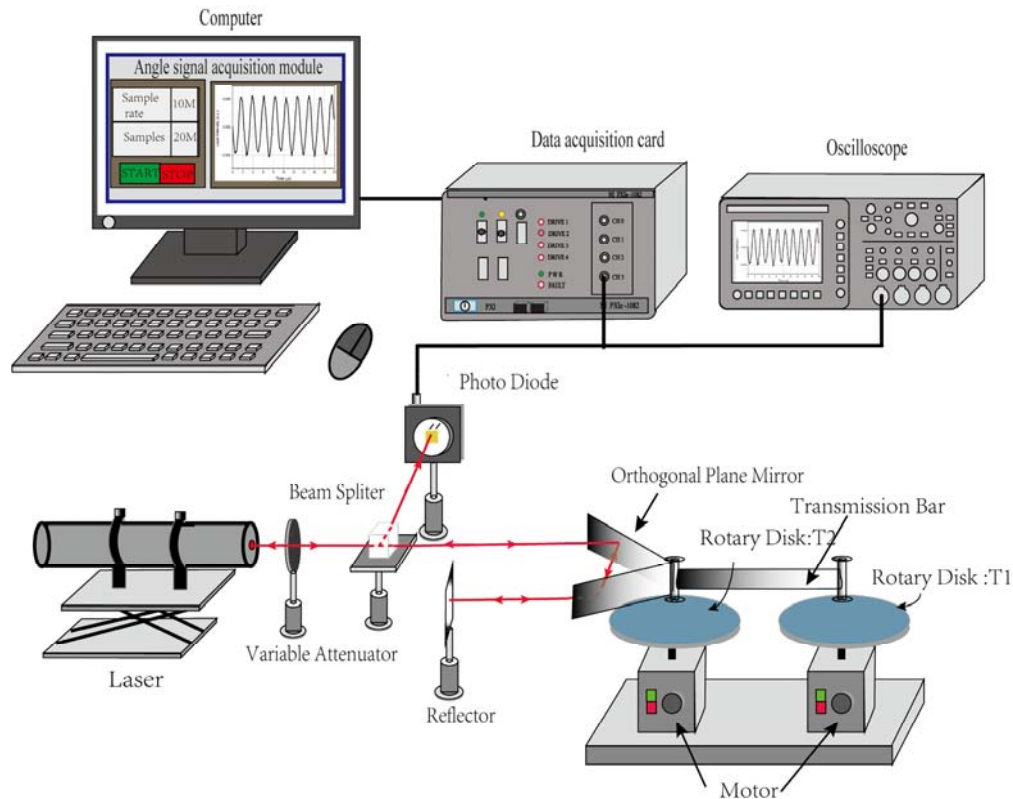


Fig. 4. Experimental setup of AM-OM-SMI system.

As shown in Fig. 4, the target that used to change the measurement angle is composed of double rotary disks and the designed mechanical linkage. Double rotary disks are driven by the any motor in below of two rotary disks. The designed mechanical linkage composed of a transmission bar, an orthogonal holder and two bearings that were fixed on the two rotary disks to ensure the orthogonal mirror rotates synchronously with the rotary disk. The two bearings are located at both ends of transmission bar to connect the rotary disks and transmission bar. When the angle changes, angular bisector of orthogonal holder is always on the same line with the transmission bar in spite of the position of designed rotary mechanical linkage changed gradually. In the same time, the instruments except rotating part are all keep still. Owing to the angular bisector of orthogonal holder is always parallel to the direction of the laser beam emitted from the laser, the beam reflected by the orthogonal mirror can incident to reflector and re-enter to the laser cavity, which solve the defect that traditional method confronted and improved the measurement range and resolution.

#### 4. Experimental results and discussion

On account of the experimental setup proposed above, we make the comparative experiment with different vertex distance. On the basis of Eq. (1) and Eq. (6), we can obtain the different resolution of angle measurement by adjusting the vertex distance. The double rotary disks and a He-Ne laser were used in AM-OM-SMI system as key component. An oscilloscope (Tektronix DPO 2024 Digital Phosphor Oscilloscope) is employed to observe the self-mixing signal related to the measured angle. The self-mixing angle signal can be acquired by data acquisition card (National Instrument PXI-1082) in whole experiment for obtain the measurement angle value. The specific self-mixing angle signal at small angle and big angle is shown in Fig. 5.

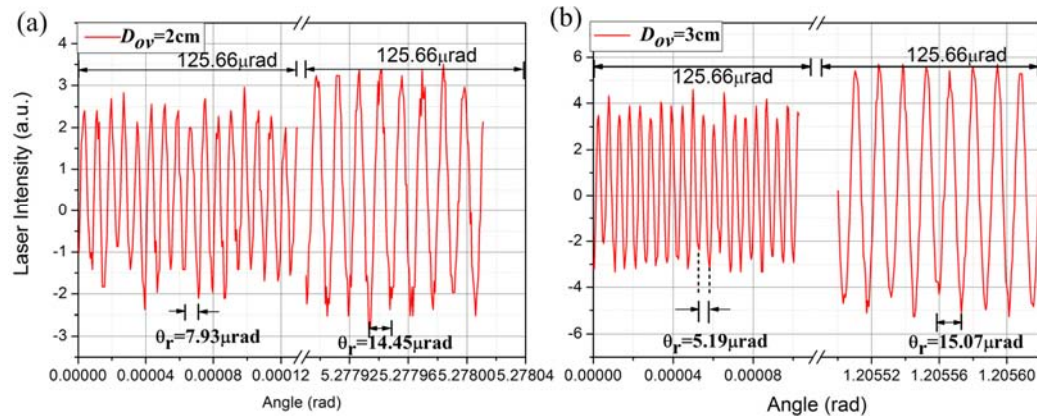


Fig. 5. The experiment results with different vertex distance. (a) the vertex distance  $D_{ov} = 2\text{ cm}$ ; (b) the vertex distance  $D_{ov} = 3\text{ cm}$ .

The Fig. 5 is the experimental signal with different vertex distance. In order to correspond to the simulate result in Fig. 2, the angle change range of experimental result shown in Fig. 5 is consistent with the theoretical simulation. From Fig. 5, it can be observed the self-mixing signal become denser with the increased vertex distance, which is in well agreement with the theoretical simulate result shown in Fig. 2. In the process of data processing, we can obtain the measurement result of different vertex distance from Fig. 5 by count the fringe number of self-mixing signal. The difference of fringe number of self-mixing signal indicates that the resolution of AM-OM-SMI system is changed. As two angle measurement resolutions in different measurement angle we marked in Fig. 5(a) and Fig. 5(b), the angle measurement resolution is  $7.93\ \mu\text{rad}$  and  $5.19\ \mu\text{rad}$  in small starting angle with the vertex distance is 2 cm and 3 cm respectively. The measurement resolution is  $14.45\ \mu\text{rad}$  and  $15.07\ \mu\text{rad}$  in big starting angle with the vertex distance is 2 cm and 3 cm respectively. It is basically consistent with the theoretical result in Fig. 2. However, there is amplitude fluctuation in Fig. 5 due to it is difficult to remain stable in experiment that there are extra vibration result from the designed mechanical linkage, which change the intensity of the light re-enter to the laser then result in the intensity of the self-mixing angle signal light is modulated. Additionally, the data acquisition card with sampling rate of 10M is used to acquire the experimental data in experiment, it also can lead to the intensity fluctuation of self-mixing angle signal because acquired data may be not enough to describe the waveform in detail.

After the comparative study of waveforms of different vertex distance of rotary disk in AM-OM-SMI system, we analyze the relationship between the fringe number and the measured angle, which is shown in Fig. 6. According to Eq. (1), the OPD caused by angle change is sine function, which shows that the frequency of self-mixing signal in measurement range is gradually changed.



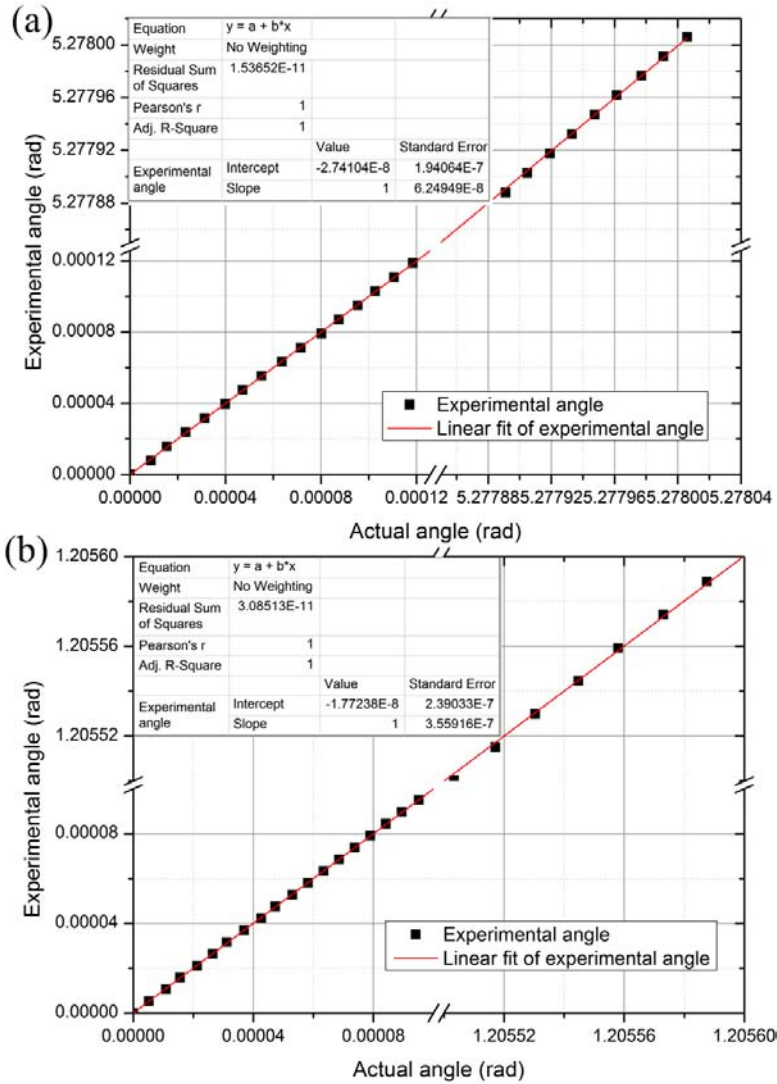


Fig. 6. Analysis diagram of different vertex distance. (a) the vertex distance  $D_{ov} = 2\text{cm}$ ; (b) the vertex distance  $D_{ov} = 3\text{cm}$ .

Figure 6 is the analysis diagram of experimental result with different vertex distance. As shown in Fig. 6, the black square dots represent the experimental result and the red line is the linear fit of experimental result. Figure 5(a) and 5(b) represent the measurement result with the vertex distance is 2 cm and 3 cm respectively. Based on the experimental results, there is a good linearity of the curves between experimental angle and actual angle with the coefficient of determination is 1. Meanwhile, it is observed that the residual sum of squares means the difference between the data point and its corresponding position on the regression line in Fig. 5(a) and Fig. 5(b) is  $1.54 \times 10^{-11}$  and  $3.09 \times 10^{-11}$  respectively. It namely the experimental result is basically consistent with the actual results. For the sake of analyze the accuracy of the experiment, we discussed the error in small angle and big angle under the same angle change range of  $125.66 \mu\text{rad}$  in Fig. 7. The spot and line graph of the upper part is the absolute error of experiment and the histogram in lower part is the relative error of experiment.

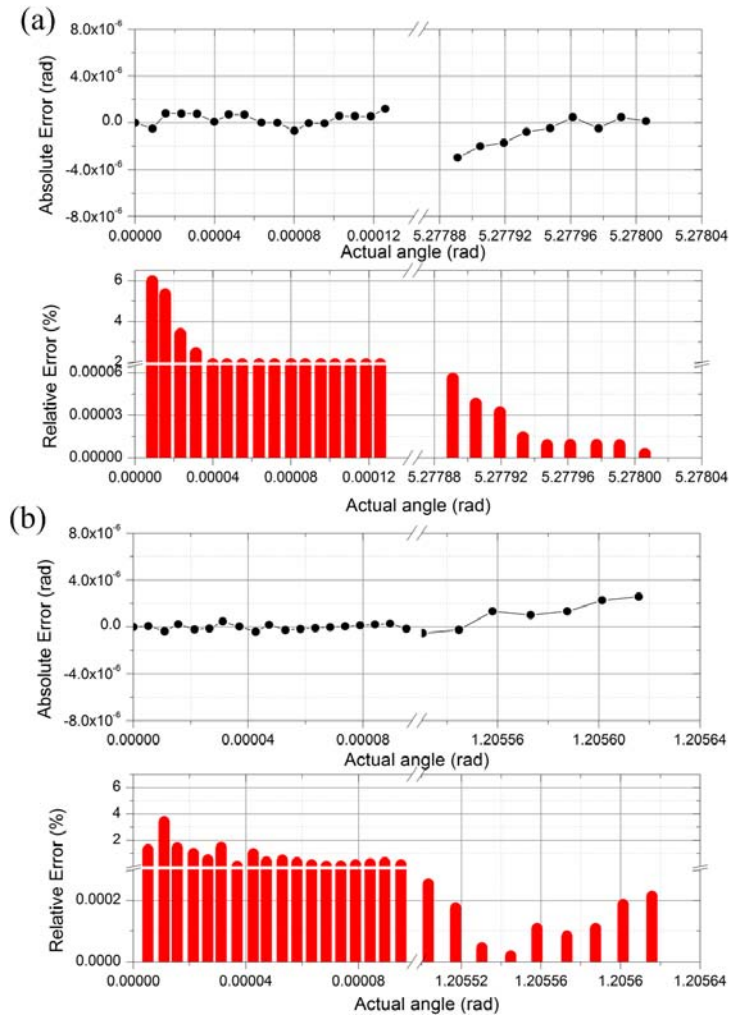


Fig. 7. Relative error and absolute error of rotating disks with different vertex distance. (a) the vertex distance  $D_{ov} = 2\text{cm}$ ; (b) the vertex distance  $D_{ov} = 3\text{cm}$ .

From Fig. 7, we can see that the absolute error in entire measured range in small angle and big angle all lower to  $\pm 2.96 \mu\text{rad}$  and  $\pm 3.06 \mu\text{rad}$  with the vertex distance of  $2\text{cm}$  and  $3\text{cm}$  respectively in measurement. The relative error is all less than  $7\%$  in experiment at any vertex distance, which is satisfied with the requirement of high-accuracy measurement. Additionally, with the increasing number of fringes, the relative error is greatly reduced and can as low as  $1 \times 10^{-4}\%$ . It greatly improved the accuracy of angle measurement in AM-OM-SMI system compared to the traditional method. However, there still exist some relative errors due to the factors such as the machining precision of the equipment, the sampling rate of data acquisition and the machining vibration caused by the rotary mechanical linkage. Therefore, the data acquisition card with bigger sampling rate and the entire experimental setup with better machining precision that can keep setup stable could be used to minimize the error of the experiment in this AM-OM-SMI system.

## 5. Conclusion

An improved angle measurement system at full-circle range with microradian resolution based on laser self-mixing effect is proposed and experimentally demonstrated in this paper.

Compared with the traditional angle measurement method, the measurement resolution and range are both greatly improved. In order to illustrate the advantage of this AM-OM-SMI system, the contrast experiment with different vertex distance is made. In contrast experiment, the resolution in this paper can reach  $7.91\mu\text{rad}$  and  $5.27\mu\text{rad}$  when vertex distance is 2cm and 3cm respectively, which shows that the larger vertex distance, the higher resolution of the angle measurement system. The absolute error can be lower to  $\pm 0.011\mu\text{rad}$  in experiment, which satisfies the requirements of most high accuracy angle measurement. Although the AM-OM-SMI system shows the better measurement resolution and accuracy contrast to the measurement resolution and error of the traditional angle measurement method with milliradian resolution, we may increase the measurement resolution further by using the phase measurement method, the laser with short wavelength, the larger vertex distance and improve accuracy by adopt the bigger sampling rate in the AM-OM-SMI system in our future works.

### Funding

National Natural Science Foundation of China (Grant No. 61307098, 61275165, 61741501); Foundation for Scientific Research and Technical Leaders in Anhui Province (Grant No. 2017H124).

### Acknowledgments

This work is supported by the National Natural Science Foundation of China (Grant No. 61307098, 61275165, 61741501), Foundation for Scientific Research and Technical Leaders in Anhui Province (2017H124).